Vol. 86 No. 3 pp. 748–761 ACTA GEOLOGICA SINICA (English Edition) June 2012

Geochronology of the Gabbro–mafic Microgranular Enclaves–granite Associations in the Gejiu District, Yunnan Province and Their Geodynamic Significance

CHENG Yanbo[1, 2] and MAO Jingwen[1, 3, *]

1 *Faculty of the Earth Sciences and Resources, China University of Geosciences, Beijing 100083*
2 *School of Earth and Environmental Sciences, James Cook University, Townsville, 4811, Australia*
3 *MLR Key Laboratory of Metallogeny and Mineral Assessment, Institute of Mineral Resources, Chinese Academy of Geological Sciences, Beijing, 100037*

Abstract: Many igneous rocks distribute in Gejiu tin polymetallic ore-field at Yunnan province, rocks including basalt, gabbro, mafic microgranular enclaves, granites (porphyritic granite and equigranular granite) and akaline rocks. The ages of the granites and akaline rocks which are considered to have genetic connecting with the mineralization have been comfirmed, but the gabbro-mafic microgranular enclaves-granite assemblage's ages are still unknown. By means of LA-ICP-MS zircon U-Pb dating, the data of Shenxianshui equigranular granite, the mafic microgranular enclave in Jiasha area, the host rock of the mafic microgranular enclaves and the Jiasha gabbro are around ~80 Ma. Besides the above mentioned data, a group of new ages at ~30 Ma were discovered in this study, which is from gabbro and mafic microgranular enclaves. Based on the previous data and the new data gained this time, we suggest the major geochronology framework of the magmatism and mineralization events in Gejiu area is ~80 Ma, which is consistent with the Late Cretaceous magmatism and mineralization events in the whole southeast Yunnan and west Guangxi area and they were suggested to belong to the same geotectonic setting in late Yenshannian. And the new ages of the ~30 Ma obtained in this study is considered to represent a responding to the complicate tectonic evolution history of the Tibetan orogenic events in Cenozoic.

Key words: gabbro, granite, mafic microgranular enclaves, geochronology, geodynamic setting, Gejiu

1 Introduction

Gabbro-granite-akaline rocks associations of which have temporal and spatial connection commonly represent an intraplate extension geodynamic setting and contain special geological significance (Abdalla et al., 1996; Cliff, 1997; Mingram et al., 2000; Grazina et al., 2003; Upadhyay et al., 2006). A suite of gabbro-mafic microgranular enclaves-granite-syenite-mafic dykes association developed in the supergiant Gejiu tin-copper metallogenic ore district (Fig. 1). As Sn mineralization always thought to be genetically related with highly fractionated granite, existing studies mainly concerned the issues of ore-related granite's petrology, evolutionary and their relationship with mineralization in Gejiu area in the past decades (308 geological Party, 1984; Li, 1985; Zhuang et al., 1996; Cheng et al., 2008a, 2008b, 2009). However, seldom studies were carried out on gabbro, MMEs and alkaline rocks, including their genesis and magmatic process, especially for their high precise ages, different authors had various ideas (308 Geological Party, 1984; Yu et al., 1988; Luo, 1995; Zhuang et al., 1996). Combined with previous data, this paper is going to report the high precise LA-ICP-MS zircon U-Pb dating results of this rock association and further discuss their special geodynamic significance.

2 Geological Background

The study area is located on the west margin of the South China block and adjacent to the Yangtze Craton in the north and to the Three Rivers fold belt in the west (inset of Fig. 1). It is bound by the Mile–Shizong fault to the north, the Ailaoshan–Honghe regional strike–slip fault

* Corresponding author. E-mail: chamboll@yahoo.cn

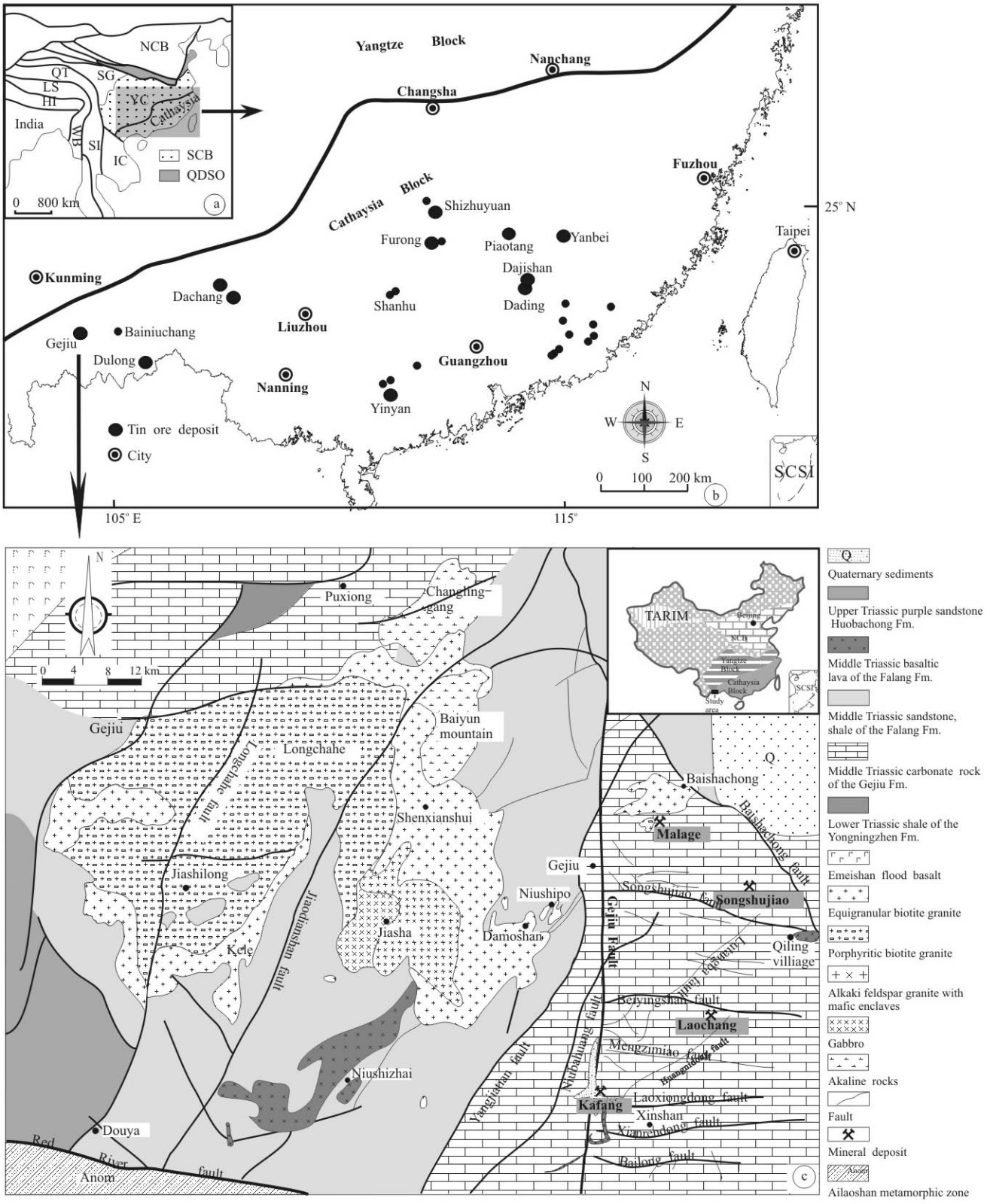

Fig. 1. (a) Simplified geological map of eastern Eurasia, showing major tectonic units (Wang et al., 2005). (b) Distribution of tin deposits in the Cathaysia block (Mao et al., 2004). (c) Sketch map showing the geology and the distribution of tin-polymetallic deposits in the Gejiu ore district (Modified from 308 Geological Party, 1984; Cheng and Mao, 2010).

SCB, South China Block; NCB, North China Block; YC, Yangtze Craton; ICB, Indochina Block; QDOB, Qinling Dabie Orogen Belt.

to the west, and the North Vietnam block in the south (inset of Fig. 1). The Gejiu district occupies about 400 km^2, and was a depression for a long time in its geological history, thus allowing the preservation of Cambrian to Quaternary successions, except for late Triassic to Cretaceous rocks, when the Gejiu district was uplifted above the sea level, due to Indosinian and Yenshannian tectonic movements. Therefore, rocks that outcrop in Gejiu area are the Middle Triassic Gejiu Formation, consisting of more than 3000 m of carbonate, and the 1800 m to 2800 m in thick Falang Formation fine-grained clastic and carbonate rocks, with the intercalated basic lavas. Numerous faults in the Gejiu area, including the NNE-trending Longchahe fault, Jiaodingshan fault, Yangjiatian fault, NE-trending Baishachong fault, and the NS-trending Gejiu fault. The Gejiu fault separates the Gejiu area into an eastern and the western sectors (Fig. 1). Late Cretaceous magmatism in the Gejiu area was very intensive and represented by various igneous rocks namely: 1) Longchahe porphyritic granite; 2) Songshujiao porphyritic granite; 3) Laochang porphyritic granite; 4) Shenxianshui equigranular granite; 5) Baishachong equigranular granite; 6) Laochang equigranular granite; 7) Xinshan equigranular granite; 8) Jiasha gabbro; 9) Jiasha mafic microgranular enclaves; 10) Baiyunshan alkaline rocks; and 11) Laochang mafic dikes. These rocks are well exposed in the western part of Gejiu area, whereas in the eastern part, they are below the surface (Fig. 1).

3 Petrography

Gabbro distributes in the southeast Longchahe porphyritic granite, occupies about 10km^2, and being surrounded by granitic rocks except its southwest part, which is hosted by the mid-Triassic Falang Formation limestone (Fig. 1). Mafic microgranular enclaves distribute in the north, east and south Jiasha gabbro stock, size ranging from 0.4 to 1.5 m (Figs. 2 and 3), and occupies 20 km^2. The host rock of the MMEs is granitoids, similar to Longchahe porphyritic granite, and the Shenxianshui equigranular granite locates in the east part. Shenxianshui granite occupies about 50 km^2, and Gejiu Formation dolomite and dolomitic limestone in its east part. Hornfels, marble and skarn can be discovered in the east and west contacts.

Jiasha gabbro is grey-black and deep green in color, fine-medium grained. Major rock-forming minerals including pyroxene (~50%) and plagioclase (~30%), accompanied by various amount of biotite and hornblende, accessory minerals include magnetite, titanite, apatite and zircon (Figs. 2 and 3). Most pyroxene are self-crystallized and coarse grained, plagioclase with zonings occasionally developed are infill in pyroxene grains. Secondary minerals, especially for K-feldspar, quartz, biotite and chlorite were extensive discovered, which were thought to be originally altered from pyroxene and hornblende (Fig. 3)

Mafic microgranular enclaves are grey and dark-green, fine-, medium– and coarse grained samples were observed in the field. Major rock-forming minerals include plagioclase, K-feldspar, biotite, hornblende, accessory minerals including apatite, titanite, allanite and zircon. Minerals content changes a lot from sample to sample, and mafic minerals ranging from 20% to 50%, and commonly extensively accompanied with biotite alteration. Minor pyroxene was found in a few areas and the content of quartz increase with the decrease of the mafic minerals.

The enclave bearing granite is pink in color and coarse granied to porphyritic texture. Minerals include plagioclase, K-feldspar, quartz, biotite, muscovite and hornblende, accessory minerals including magnetite, apatite, zircon, fluorite and tourmaline. Plagioclase is self-crystallized and reaches up to 50% at most, and their sizes are about 6 mm to 1 cm in length, with a few K-feldspar and quartz inclusions. Some plagioclases are extensive altered to be sericite.

4 Analytical Methods and Results

4.1 Analytical techniques

Zircons were separated from 5–15 kg crushed granite, gabbro and enclave samples, using conventional heavy liquid and magnetic techniques. Representative zircon grains were handpicked under binocular microscope, mounted in epoxy resin, polished and coated with gold. The mounts were photographed in transmitted and reflected light, and cathodoluminescence (CL) images obtained using a JEOL-JXA–8800 microprobe were used to examine the internal structure of analyzed zircons. In order to eliminate the influence of Common Pb, the gold coating was removed prior to U-Pb analyses.

U-Pb dating of zircons was conducted by LA-MC-ICP-MS at the Institute of Mineral Resources, Chinese Academy of Geological Sciences, Beijing. Detailed operating conditions for the laser ablation system and the MC-ICP-MS instrument and data reduction were the same as described by Hou et al. (2009). Laser sampling was performed using a New-wave UP213 laser ablation system. Helium was applied as a carrier gas to the ablation chamber. Argon was used as the make-up gas and mixed with the carrier gas via a T-connector before entering the ICP-MS. A Thermo Finnigan Neptune MC-ICP-MS instrument was used to acquire ion-signal intensities. The array of four multi-ion-counters and three faraday cups

Fig. 2. Photos of the gabbro-mafic microgranular enclaves in Gejiu area.
(a) and (b) are specimen photos of the mafic microgranular enclaves; (c) is the photo of the Jiasha gabbro, and (d) is showing a k-rich felsic vein cut the Jiasha gabbro.

allowed for simultaneous detection of ^{202}Hg (on IC5), ^{204}Hg, ^{204}Pb (on IC4), ^{206}Pb (on IC3), ^{207}Pb (on IC2), ^{208}Pb (on L4), ^{232}Th (on H2), ^{238}U (on H4) ion signals. Each analysis incorporated a background acquisition of approximately 20–30 s (gas blank) followed by 30 s data acquisition from the sample. Off-line raw data selection and integration of background and analyte signals, and time-drift correction and quantitative calibration for U-Pb dating, was performed by ICPMSDataCal (Liu et al. 2010).

Zircon GJ1 was used as external standard for U-Pb dating, and was analyzed twice for every 5–10 analyses of zircon samples. Time-dependent drifts of U-Th-Pb isotopic ratios were corrected using a linear interpolation for every batch of bracketed analyses according to the variations of GJ1 (Liu et al. 2010). U-Th-Pb isotopic ratios used for GJ1 are from Jackson et al. (2004). Uncertainties of preferred values for the external standard GJ1 were within the expected error range. In all analyzed zircon grains the common Pb correction was not necessary due to the low signal of common ^{204}Pb and high ^{206}Pb/^{204}Pb. Uranium, Th and Pb concentrations were determined using zircon M127 (Nasdala et al. 2008) as an external standard. Concordia diagrams and weighted mean calculations were made using Isoplot/Exver3 (Ludwig 2003). Errors on individual analyses by LA-MC-ICP-MS are quoted at the 95% (1σ) confidence level. The zircon Plesovice was dated as a secondary standard and yielded a weighted mean of ^{206}Pb/^{238}U age of 337±2 Ma (2SD, n=12), which conforms to the recommended ^{206}Pb/^{238}U age of 337.13±0.37 Ma (Sláma et al. 2008).

4.2 Results

Zircons from the Shenxianshui granite, Jiasha gabbro, Jiasha mafic microgranular enclaves, granite which close to the MMEs distributing area, and enclave-bearing granite were picked up for LA-ICP-MS U-Pb zircon dating. Size and shape of zircons from these samples various a lot, and cathodoluminescence images show that they are generally embayed with some cracks, and part of grains have micro-scale, magmatic oscillatory zonings (Fig. 4), but the rest of them with few or ambiguous zonings, indicating a metamorphic origin (Wu, 2004). The age of each sample is given by the error-weighted mean of

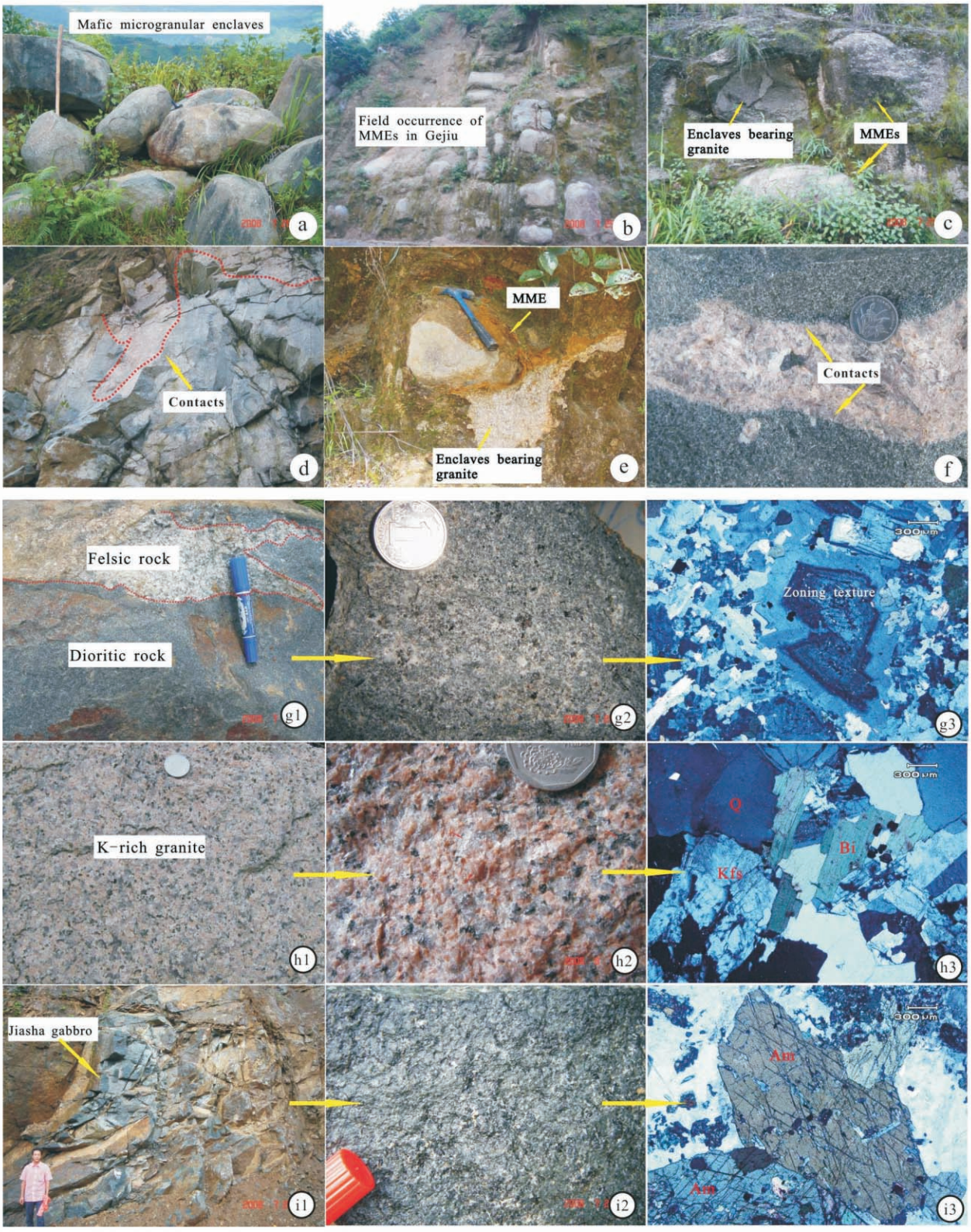

Fig. 3. Field geological character of the gabbro-dioritic xenoliths-granite in Gejiu area.

the common Pb-corrected $^{206}Pb/^{238}U$ ages of the selected grains at 95% confidence level. U-Pb data sets for all samples are given in Table 1.

4.2.1 Shenxianshui granite (CYB0707020 and CYB0807030)

By means of LA-ICP-MS, zircons from sample (CYB0707020) from Shenxianshui equigranular granite

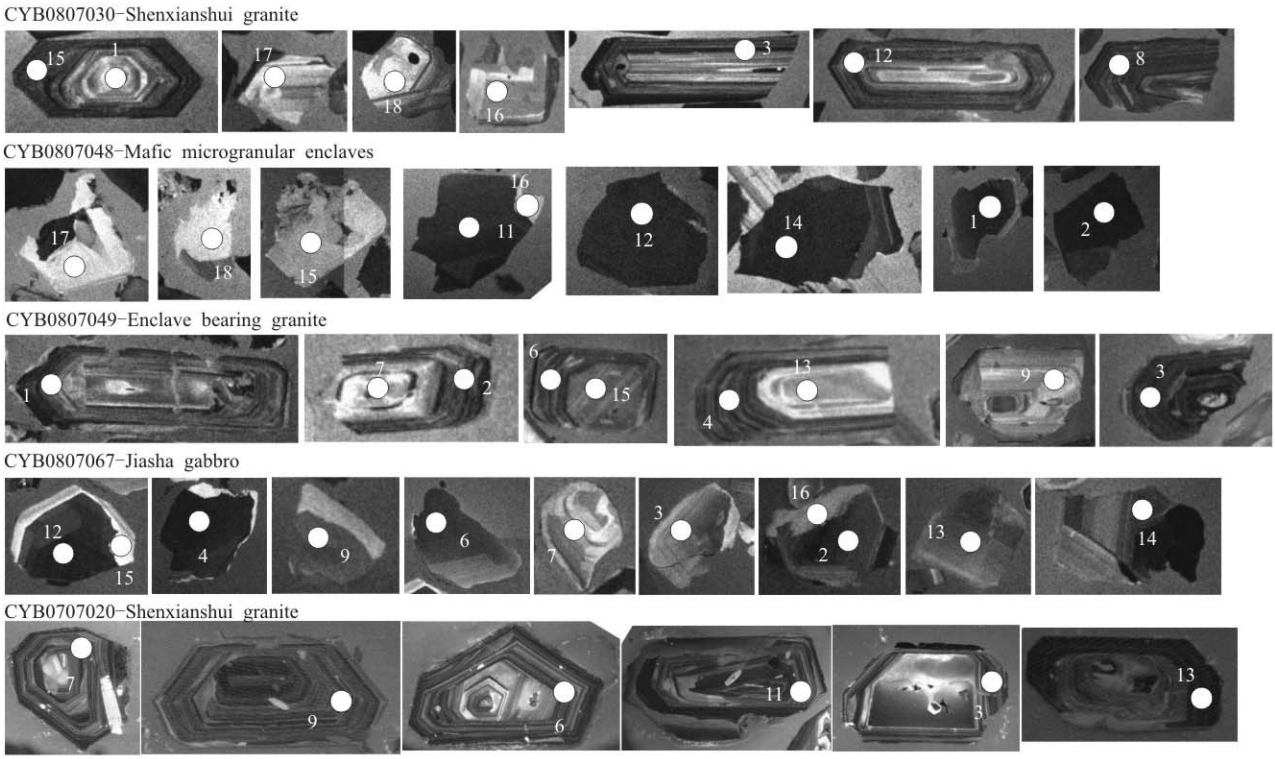

Fig. 4. Internal structure of zircon grains shown by cathodoluminescence analysis.

were analyzed and 13 groups of data were obtained and yield a $^{206}Pb/^{238}U$ weighted mean age of 83±0.35 Ma, with MSWD=1.19 and the ratio of Th/U is from 0.11 to 1.05 with average value 0.46 (2σ; Table 1 and Fig. 5). Meanwhile, we also analyzed another 20 spots from sample CYB0807030 collected from Shenxianshui granite, the results of which were divided into two groups. The first group is close to ~80 Ma, and the ratio of Th/U is range from 0.78 to 2.70 and the average value is 1.24, furthermore, the zircons of this group are bright or yellowish and oscillatory zonings are well developed, indicating a magmatic origin. Concordant ages from 79 to 85 Ma with a weighted mean of 81±0.7 Ma were obtained, with MSWD=2.8 (2σ; Table 1; Fig. 5). The data of this group is given by the error-weighted mean of the common Pb-corrected $^{206}Pb/^{238}U$ ages of the selected grains at 95% confidence level. U-Pb data sets for all samples are given in Table 1. Another group of ages are much younger than the previous one. The $^{206}Pb/^{238}Pb$ weighted mean age is 30±0.88 Ma and the MSWD is 2.9. The analysis spots of this group locate in the margin of zircons, more over, the color of these areas are much darker, indicating high U and Th contents. The variation of Th/U ratio is larger, which range from 0.11 to 0.84 with average value 0.37 (> 0.4), indicating a metamorphic origin.

4.2.2 Mafic microgranular enclaves (CYB0807048)

Two groups of age data were obtained from eighteen analyzed spots on 14 zircon grains from the Jiasha enclaves, which is consistent with the characteristics of the color and texture of the zircon from these enclaves (Fig. 4). Core area and margin area exhibit obvious difference in CL image in part of zircons indicating the origin of these zircons are not only magmatic but metamorphic process maybe also played an important role. The four analysis spots locate in the core area yield a $^{206}Pb/^{238}U$ weighted mean age of 82±0.0 Ma, with MSWD=1.3 (2σ; Table 1 and Fig. 5), and their Th/U ratio is from 0.30 to 0.47 with average value of 0.38. This data is considered to be the crystallization age of these enclaves. As mentioned above, another 14 analysis spots on the zircon margin have large Th/U ratio range (0.17–1.67) indicating they are not a single magmatic origin. The $^{206}Pb/^{238}U$ weighted mean age of this group is 30±0.53 Ma and the MSWD value is 0.92.

4.2.3 Enclave bearing granite (CYB0807049)

The enclave bearing rock is alkaline-rich granite. Sixteen spots on 13 zircon grains from this rock were analyzed and their data exhibits excellent consistency (Fig. 5). Similar to the former samples, the results of this sample also can be divided into two groups, which is consistent with their color and micro-texture from CL images. Ten of the 16 spots, which are locate in the core area of the analyzed zircons, have a $^{206}Pb/^{238}U$ weighted mean age of 81±0.52 Ma with MSWD value is 0.51, and

Table 1 Zircon U-Pb dating of gabbro-mafic microgranular enclaves-granite assemblage in Gejiu area Shenxianshui granite (CYB0707020)

Spot	Th (ppm)	U (ppm)	Th/U	$^{207}Pb/^{206}Pb$	1σ	$^{207}Pb/^{235}U$	1σ	$^{206}Pb/^{238}U$	1σ	$^{208}Pb/^{232}U$	1σ	*t* (Ma)
1	1212	4019	0.3016	0.0502	0.0009	0.0917	0.0010	0.0132	0.0001	0.0040	0.0000	85
2	1134	1247	0.9094	0.0440	0.0009	0.0796	0.0012	0.0131	0.0001	0.0036	0.0000	84
3	3695	9798	0.3771	0.0719	0.0014	0.1300	0.0022	0.0131	0.0001	0.0040	0.0000	84
4	923	2999	0.3078	0.0511	0.0016	0.0907	0.0027	0.0129	0.0001	0.0041	0.0001	82
5	1649	1567	1.0521	0.0581	0.0028	0.1022	0.0048	0.0128	0.0002	0.0040	0.0000	82
6	546	1403	0.3890	0.0601	0.0046	0.1093	0.0082	0.0132	0.0002	0.0041	0.0001	84
7	217	749	0.2900	0.0480	0.0019	0.0865	0.0033	0.0131	0.0002	0.0042	0.0001	84
8	901	1537	0.5859	0.0701	0.0022	0.1273	0.0038	0.0132	0.0002	0.0040	0.0000	84
9	1888	3502	0.5391	0.0684	0.0029	0.1210	0.0050	0.0128	0.0002	0.0039	0.0001	82
10	2067	6669	0.3099	0.0587	0.0026	0.1059	0.0046	0.0131	0.0001	0.0041	0.0001	84
11	1084	4125	0.2628	0.0510	0.0013	0.0905	0.0021	0.0129	0.0001	0.0041	0.0001	82
12	1223	2376	0.5148	0.0580	0.0018	0.1026	0.0030	0.0128	0.0001	0.0040	0.0000	82
13	517	4348	0.1190	0.0424	0.0009	0.0765	0.0010	0.0131	0.0001	0.0040	0.0001	84
Granite close to MME-distributing area (CYB0807030)												
Spot	Th (ppm)	U (ppm)	Th/U	$^{207}Pb/^{206}Pb$	1σ	$^{207}Pb/^{235}U$	1σ	$^{206}Pb/^{238}U$	1σ	$^{208}Pb/^{232}U$	1σ	*t* (Ma)
1	4668	10117	0.46	0.0462	0.0013	0.0304	0.0007	0.0048	0.0001	0.0015	0.0000	31
2	5992	17633	0.34	0.0474	0.0013	0.0305	0.0007	0.0047	0.0001	0.0015	0.0000	30
3	967	3802	0.25	0.0570	0.0017	0.0385	0.0011	0.0049	0.0001	0.0046	0.0003	31
4	5166	9921	0.52	0.0498	0.0008	0.0328	0.0005	0.0048	0.0001	0.0016	0.0001	31
5	2098	10749	0.20	0.0506	0.0008	0.0330	0.0006	0.0047	0.0001	0.0029	0.0001	30
6	3725	4439	0.84	0.0499	0.0010	0.0336	0.0007	0.0049	0.0001	0.0018	0.0001	31
7	4693	6554	0.72	0.0461	0.0010	0.0308	0.0006	0.0048	0.0001	0.0016	0.0001	31
8	2990	11132	0.27	0.0461	0.0016	0.0286	0.0009	0.0045	0.0001	0.0015	0.0001	30
9	1004	6849	0.15	0.0576	0.0008	0.0377	0.0006	0.0048	0.0001	0.0050	0.0002	31
10	947	6116	0.15	0.0565	0.0010	0.0366	0.0006	0.0047	0.0001	0.0046	0.0002	30
11	6686	35524	0.19	0.0466	0.0017	0.0299	0.0010	0.0047	0.0001	0.0015	0.0001	30
12	977	8601	0.11	0.0686	0.0014	0.0470	0.0010	0.0050	0.0001	0.0086	0.0009	32
13	2889	4013	0.72	0.0461	0.0016	0.0308	0.0009	0.0049	0.0001	0.0029	0.0007	31
14	4193	9367	0.45	0.0499	0.0025	0.0342	0.0016	0.0050	0.0001	0.0016	0.0000	32
15	269	333	0.81	0.0497	0.0015	0.0893	0.0027	0.0130	0.0002	0.0042	0.0002	83
16	592	642	0.92	0.0521	0.0020	0.0937	0.0035	0.0130	0.0002	0.0045	0.0004	83
17	285	304	0.94	0.0671	0.0081	0.1235	0.0146	0.0134	0.0003	0.0041	0.0001	85
18	1094	405	2.70	0.0489	0.0024	0.0853	0.0040	0.0126	0.0003	0.0041	0.0003	81
19	638	815	0.78	0.0461	0.0051	0.0780	0.0086	0.0123	0.0002	0.0040	0.0004	79
20	609	472	1.29	0.0461	0.0065	0.0795	0.0111	0.0125	0.0002	0.0042	0.0004	80
Microgranular mafic enclave (CYB0807048)												
Spot	Th (ppm)	U (ppm)	Th/U	$^{207}Pb/^{206}Pb$	1σ	$^{207}Pb/^{235}U$	1σ	$^{206}Pb/^{238}U$	1σ	$^{208}Pb/^{232}U$	1σ	*t* (Ma)
1	17024	23541	0.72	0.0485	0.0006	0.0314	0.0004	0.0047	0.0001	0.0016	0.0001	30
2	1063	4878	0.22	0.0485	0.0008	0.0320	0.0005	0.0048	0.0001	0.0043	0.0001	31
3	1397	8350	0.17	0.0500	0.0007	0.0324	0.0005	0.0047	0.0001	0.0042	0.0001	30
4	652	3092	0.21	0.0508	0.0014	0.0336	0.0009	0.0048	0.0001	0.0043	0.0002	31
5	10886	8266	1.32	0.0491	0.0007	0.0326	0.0005	0.0048	0.0001	0.0016	0.0001	31
6	7125	8957	0.80	0.0461	0.0015	0.0301	0.0009	0.0047	0.0001	0.0015	0.0000	31
7	1372	7258	0.19	0.0484	0.0007	0.0321	0.0005	0.0048	0.0001	0.0038	0.0001	31
8	16273	13911	1.17	0.0485	0.0006	0.0322	0.0005	0.0048	0.0001	0.0015	0.0000	31
9	30617	23889	1.28	0.0488	0.0006	0.0314	0.0004	0.0047	0.0001	0.0014	0.0000	30
10	16991	10201	1.67	0.0476	0.0006	0.0315	0.0005	0.0048	0.0001	0.0014	0.0000	31
11	26033	17197	1.51	0.0501	0.0006	0.0325	0.0005	0.0047	0.0001	0.0014	0.0000	30
12	15531	25171	0.62	0.0484	0.0006	0.0315	0.0004	0.0047	0.0001	0.0015	0.0000	30
13	15291	12555	1.22	0.0487	0.0006	0.0318	0.0005	0.0047	0.0001	0.0015	0.0000	30
14	11250	16318	0.69	0.0466	0.0016	0.0299	0.0010	0.0047	0.0001	0.0015	0.0000	30
15	167	431	0.39	0.0463	0.0019	0.0807	0.0031	0.0126	0.0002	0.0040	0.0002	81
16	133	446	0.30	0.0474	0.0018	0.0829	0.0030	0.0127	0.0002	0.0040	0.0001	81
17	280	600	0.47	0.0539	0.0012	0.0962	0.0022	0.0130	0.0002	0.0055	0.0002	83
18	211	615	0.34	0.0507	0.0012	0.0906	0.0021	0.0130	0.0002	0.0050	0.0002	83
Enclave bearing granite (CYB0807049)												
Spot	Th (ppm)	U (ppm)	Th/U	$^{207}Pb/^{206}Pb$	1σ	$^{207}Pb/^{235}U$	1σ	$^{206}Pb/^{238}U$	1σ	$^{208}Pb/^{232}U$	1σ	*t* (Ma)
1	2020	8876	0.23	0.0538	0.0008	0.0353	0.0006	0.0048	0.0001	0.0035	0.0001	30.6
2	624	5515	0.11	0.0491	0.0012	0.0324	0.0008	0.0048	0.0001	0.0039	0.0002	30.8
3	464	5292	0.09	0.0498	0.0010	0.0329	0.0007	0.0048	0.0001	0.0042	0.0002	30.8
4	623	3120	0.20	0.0533	0.0019	0.0358	0.0013	0.0049	0.0001	0.0045	0.0002	31.3
5	532	2659	0.20	0.0559	0.0016	0.0374	0.0011	0.0049	0.0001	0.0039	0.0002	31.2
6	705	3348	0.21	0.0477	0.0012	0.0318	0.0008	0.0048	0.0001	0.0039	0.0001	31.1
7	276	812	0.34	0.0482	0.0017	0.0848	0.0030	0.0128	0.0002	0.0041	0.0002	82

Table 1 continued

Enclave bearing granite (CYB0807049)

Spot	Th (ppm)	U (ppm)	Th/U	$^{207}Pb/^{206}Pb$	1σ	$^{207}Pb/^{235}U$	1σ	$^{206}Pb/^{238}U$	1σ	$^{208}Pb/^{232}U$	1σ	*t* (Ma)
8	88	85	1.04	0.0480	0.0049	0.0852	0.0084	0.0129	0.0004	0.0048	0.0004	83
9	133	92	1.44	0.0477	0.0052	0.0842	0.0088	0.0128	0.0004	0.0043	0.0003	82
10	320	205	1.56	0.0480	0.0040	0.0857	0.0070	0.0129	0.0003	0.0038	0.0002	83
11	260	292	0.89	0.0485	0.0019	0.0854	0.0032	0.0128	0.0002	0.0040	0.0002	82
12	601	689	0.87	0.0483	0.0012	0.0845	0.0021	0.0127	0.0002	0.0044	0.0002	81
13	194	230	0.85	0.0551	0.0027	0.0964	0.0046	0.0127	0.0003	0.0041	0.0002	81
14	669	684	0.98	0.0499	0.0036	0.0856	0.0059	0.0125	0.0002	0.0039	0.0001	80
15	277	640	0.43	0.0482	0.0027	0.0843	0.0045	0.0127	0.0003	0.0037	0.0003	81
16	415	351	1.18	0.0477	0.0013	0.0842	0.0023	0.0128	0.0002	0.0037	0.0001	82

Jiasha Gabbro (CYB0807067)

Spot	Th (ppm)	U (ppm)	Th/U	$^{207}Pb/^{206}Pb$	1σ	$^{207}Pb/^{235}U$	1σ	$^{206}Pb/^{238}U$	1σ	$^{208}Pb/^{232}U$	1σ	*t* (Ma)
1	7606	6287	1.21	0.0491	0.0007	0.0327	0.0005	0.0048	0.0001	0.0015	0.0000	31
2	21653	10326	2.10	0.0497	0.0006	0.0328	0.0005	0.0048	0.0001	0.0014	0.0000	31
3	24679	12376	1.99	0.0482	0.0006	0.0316	0.0005	0.0048	0.0001	0.0014	0.0000	31
4	1252	7823	0.16	0.0540	0.0009	0.0348	0.0006	0.0047	0.0001	0.0042	0.0001	30
5	10785	9407	1.15	0.0509	0.0008	0.0333	0.0005	0.0047	0.0001	0.0015	0.0000	31
6	9760	6986	1.40	0.0475	0.0007	0.0311	0.0005	0.0048	0.0001	0.0014	0.0000	31
7	11867	8351	1.42	0.0479	0.0007	0.0314	0.0005	0.0048	0.0001	0.0014	0.0000	31
8	11394	8748	1.30	0.0491	0.0008	0.0322	0.0005	0.0048	0.0001	0.0015	0.0000	31
9	1475	3337	0.44	0.0531	0.0013	0.0356	0.0009	0.0049	0.0001	0.0038	0.0002	31
10	1082	5628	0.19	0.0561	0.0009	0.0373	0.0006	0.0048	0.0001	0.0046	0.0002	31
11	1513	4082	0.37	0.0491	0.0011	0.0324	0.0007	0.0048	0.0001	0.0037	0.0001	31
12	15762	8445	1.87	0.0589	0.0010	0.0394	0.0007	0.0048	0.0001	0.0015	0.0001	31
13	1198	11180	0.11	0.0626	0.0017	0.0416	0.0011	0.0048	0.0001	0.0070	0.0003	31
14	8294	9731	0.85	0.0602	0.0011	0.0391	0.0007	0.0047	0.0001	0.0016	0.0001	30
15	568	665	0.85	0.0522	0.0053	0.0914	0.0091	0.0127	0.0003	0.0040	0.0001	81
16	415	869	0.48	0.0500	0.0029	0.0861	0.0048	0.0125	0.0002	0.0039	0.0001	80

this data is considered to be the crystallization age of the enclave bearing granite (Fig. 4). The Th/U ratio of this group data is ranging from 0.34 to 1.44, with average value is 0.96, keeping consistent with characteristics of the magmatic origin zircon. Six analysis spots on the margin of zircon grains have lower Th/U ratio of 0.09–0.23 with average of 0.17, close to the range of metamorphic zircon and indicating a non-magmatic origin. The $^{206}Pb/^{238}U$ weighted mean age of this group data is 30±0.95 Ma, and the MSWD value is 0.41.

4.2.4 Gabbro (CYB0807067)

Sixteen spots on 14 zircon grains from Jiasha gabbro were analyzed and their concordant diagram exhibits excellent consistency (Fig. 5). Similar to the former samples, the ages of this sample lies into two groups, and their $^{206}Pb/^{238}Pb$ weighted mean ages are 80±0.20 Ma and 30±0.90 Ma, with MSWD values are 0.20 and 0.74, respectively. The Th/U ratio of the former sample is ranging from 0.11 to 2.10 with average value is 0.68, and Th/U ratio of the latter one is from 0.11 to 2.10 with average of 1.04. Based on their micro-textures from the CL images (Fig. 4), the crystallization age of Jiasha gabbro is 80±0.20 Ma, and the age of 30±0.90 Ma represent the timing of a later re-heat and metamorphic event.

A special characteristic of the data in this study is all the ages in each sample can be divided into two groups, i.e., ~80 Ma and ~30 Ma (Fig. 5), more importantly, each group shows excellent consistency, indicating the data of this study is reliable.

5 Discussion

5.1 Timing of the gabbro-enclaves-granite association

As shown in the Figure 1, the Jiasha gabbro locates in the east of the Shenxianshui granite and the MMEs are distributing between the granite and gabbro. More enclaves in the area close to gabbro and getting less close to granite. The enclave bearing granite is alkaline rich and coarse grained, and the size of the enclaves is different. The MMEs have various shapes and the largest ones reach up to 2 meters across (Fig. 2). Commonly the contact between the MMEs and its host granite is sharp (Figs. 2 and 3) and irregular and the margins are darker and finer-grained margins than in the internal zone of the enclave (Figs. 2 and 3).

In this study, we obtained the age of the Shenxianshui equigranular granite in Gejiu district, Yunnan provice is during 81±0.7 to 83±0.4 Ma, the mafic microgranular enclaves is in 82±0.0 Ma, the enclave bearing granite is in 81±0.5 Ma and the Jiasha gabbro is in 80±0.2 Ma. Previous studies reported the timing of the magmatism and mineralization events in the Gejiu district is during 77

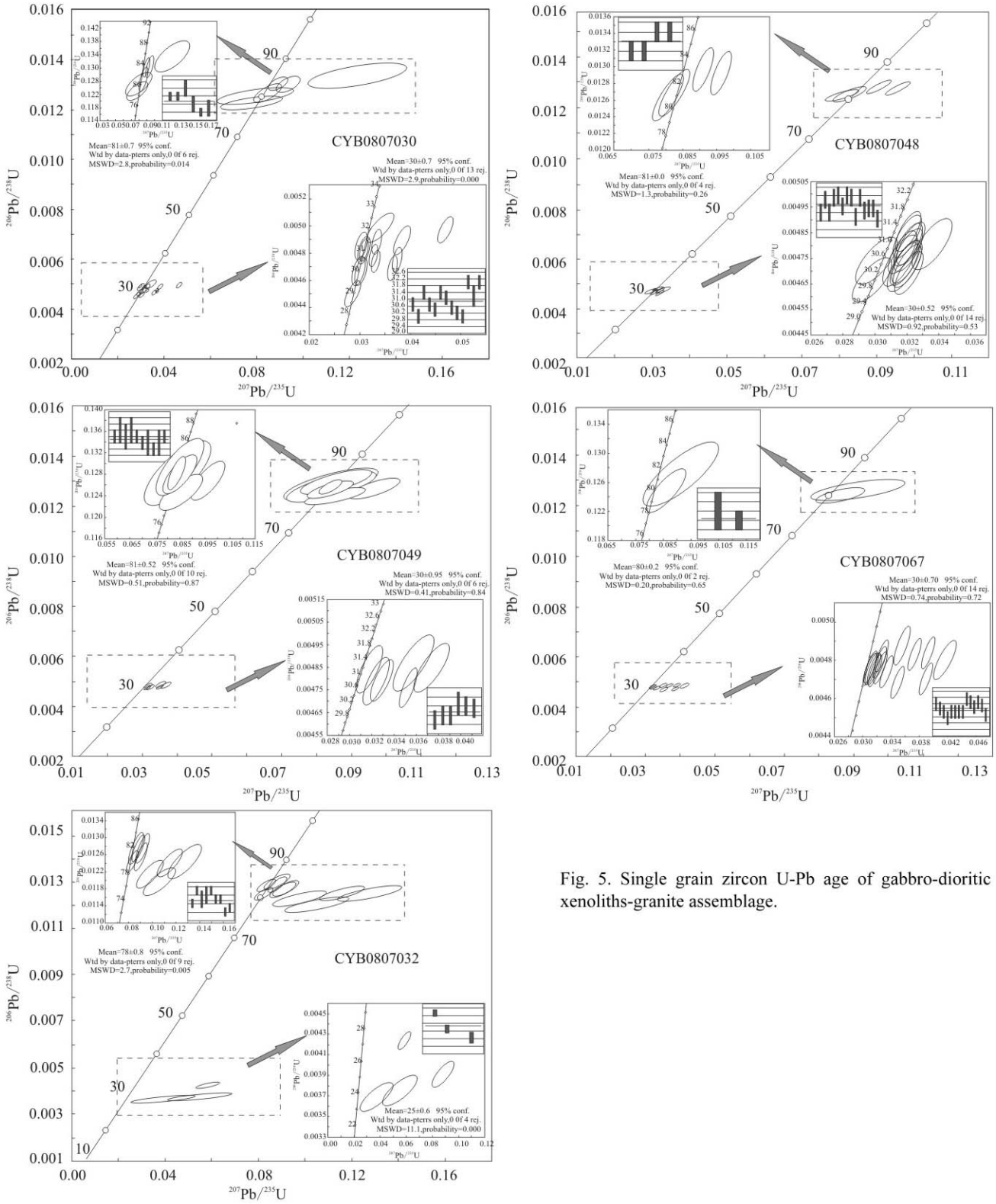

Fig. 5. Single grain zircon U-Pb age of gabbro-dioritic xenoliths-granite assemblage.

Ma to 85 Ma (Cheng et al., 2010, 2012a, 2012b), which are consistent with the results of this study and indicating these ages are reliable and can be considered to be the crystallization age of these rocks. Meanwhile, the ages of ~30 Ma in this study is considered to represent the timing of later thermal event. First, the analyzed spots of the ~80 Ma ages locate in the core area the zircons, which are commonly brighter as the low concentration of Th and U contents and high U/Th ratio. However, the analyzed spots of the ~30 Ma are on the margin of zircons, and these areas are darker as high concentrations of Th and U bu low U/Th ratios. This means later heats caused the re–

allocation of U-Th-Pb systems and thus lead the concentrate of U and Th on the margin of these zircons (Vavra et al., 1990; Rizvanova et al., 2000; Crofu et al., 2003). Therein, the maximum age of the zircons which were not influenced by metamorphism commonly represent the crystallization age of the rocks, while the minimum age of these zircons is the timing of re-crystallization caused by latter metamorphic fluids (Vavra, 1990; Hoskin, 2000). Obviously, the zircons from the gabbro, mafic microgranular enclaves and the granites in the Gejiu district have the characteristics of metamorphic zircon, and we assume this was caused by the re-heat of latter metamorphic fluids and lead the zircons re-crystallization, which mainly influenced the margin of these zircons but put little effect on the core area. Hence, the ages of the core area in zircons from the gabbro, enclaves and granite in the Gejiu district represent the crystallization age of these rocks.

5.2 30 Ma: Responses to the collision between India Plate and Euroasian continent in Cenozoic

Spatially, Gejiu district is close to the Red River-Ailaoshan metamorphic and fold belt, thus many authors tried to find out the geotectonic influence on the western South China Block from the Tethys domain (308 Geological Party, 1984; Wang, 2006), however, seldom connections were discovered in the past. From 1990s, a Cenozoic alkaline-rich intrusive rocks belt was reported, which formed during 27 to 41 Ma and starts from Aolaoshan-Jinshajiang in the south, to Yushu and Hoh Xil in the meddle, reach Tashkurghan in Xinjiang province in the north, extends 3700 km (Zhang et al., 1997). During the past 20 years' study, this belt was confirmed and more discoveries and understandings were reported, which is thought to be the result of the collision between India Plate and Euroasian continent (Zhang et al., 1997; Chung et al., 1998; Deng et al., 1998; Wang et al., 2001; Wang et al., 2001, 2002; Liu et al., 2003; Lin et al., 2005; Xia et al., 2005; Liang et al., 2006; Mo et al., 2007), and further classified this belt into 7 alkaline rock concentration areas (Fig. 6). Except the seventh area in the southernmost, the timing of other six areas is similar, which is from 26 Ma to

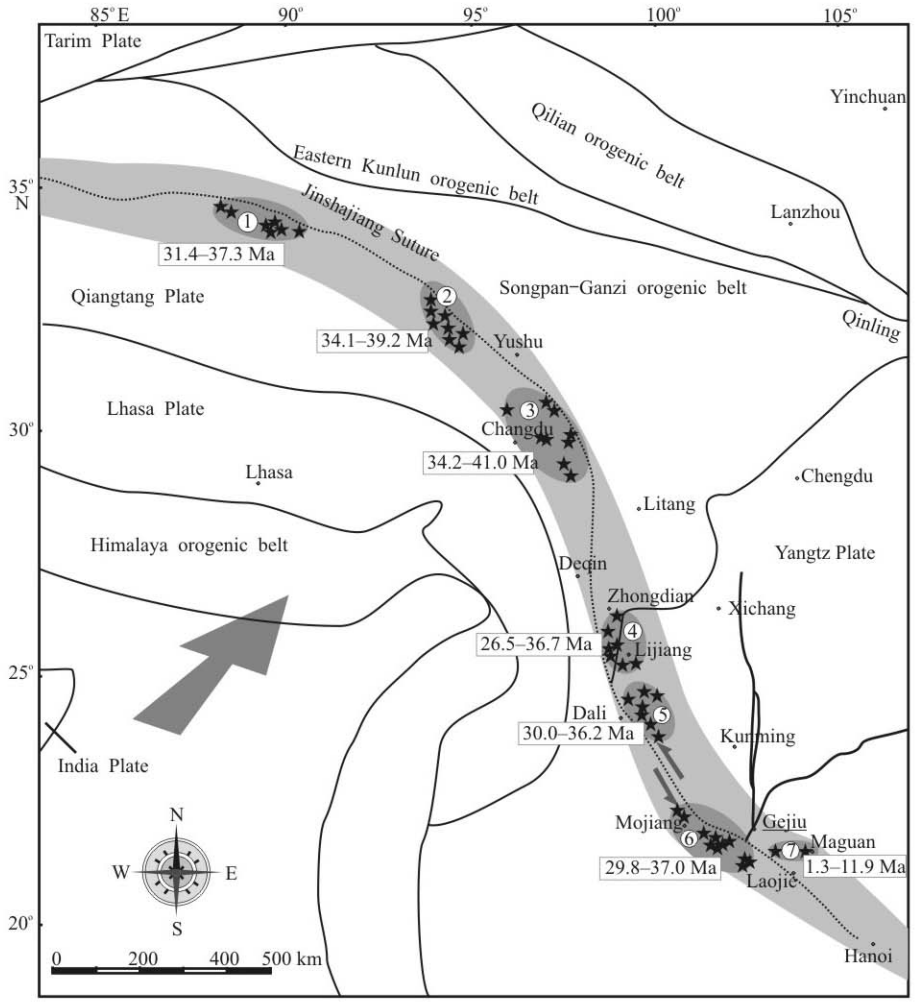

Fig. 6. The distribution of the Cenozoic magma-mineralization event along the Jinsha suture-Litang fault-Honghe fault belt.

41 Ma, and existing studies argued this belt is the responses to the collision between India Plate and Euroasian continent in Cenozoic. Although most of these areas are locate in the western of Red River Fault, the fourth and fifth areas are in the east, and specially, the seventh area, which locates in the south of Gejiu area and formed during 1.3 Ma to 11.9 Ma, also in the east of Red River Fault (Fig. 6). The above data indicates that the influence of the collision between India Plate and Euroasian continent is from 40 Ma to 1.3 Ma and geographically, it affected the both sides of the Red River Fault. This understanding is consistent with the result of this study, and indicates the ~30 Ma ages in the Gejiu district are not occasional but part of the large scale Cenozoic geotectonic-thermal event along the Jinshajiang Suture and Red River Fault (Fig. 7).

5.3 Evolution of the geodynamic process in Gejiu district from Late Cretaceous to Cenozoic

Previous studies reported the obvious temporal and spatial difference between western South China Block tin belt and western Yunnan Province tin belt, and further discussed their distinguished geodynamic setting and mineralization process (Cheng et al., 2009). During Late Cretaceous, extensional structures, which including detachment belt in different stratigraphic layers, metamorphic core complex and pull-apart basins, well developed in the western South China Block, especially in southeast Yunnan province and western Guangxi province (Mao et al., 2008b, 2008c). These contemporaneous extensional structures were considered to be controlled by a similar geodynamic mechanism. The mineralization reflection of this Late Cretaceous large scale lithospheric extension in western South China Block is the formation of a group of world class granite-related tin polymetallic deposits during 80 to 100 Ma, including Gejiu, Dachang, Dulong, etc.(Mao et al., 2008b; Cheng et al., 2010, 2012a, 2012b). Faults and fractures in crust in this district were activated by this regional extension and afterwards acted as the conduits of the mafic, intermediate and felsic magmas and following emplacement, which formed this bimodal intrusive rocks association in Gejiu district.

Ailaoshan-Red River Fault is one of the most important regional structures in SE Asia. As the convergence of the India Plate and Euroasian continent, the Ailaoshan-Red River Fault was activated and experienced left-lateral strike-slip, which happened during ~34 to ~17 Ma (Tapponnier et al., 1990; Harrison et al., 1996; Ratschbacher et al., 1996; Wang et al., 1998; Leloup et al., 2001; Gilley et al., 2003). It is possible that the new ages of ~30 Ma reported in this study is the result of the left-lateral strike-slip of Ailaoshan-Red River Fault, which is favor for the migration of heat and fluids (Fig. 7). These Cenozoic fluids renovated the ~80 Ma formed intrusive rocks and caused the re-growth of zircon, and lead the shape and color of these zircons re-worked (Fig. 4). In summary, this group of ~30 Ma data obvious show that the the evidence of the collision between India Plate and Euroasian continent influenced the igneous rocks in Gejiu district, which locates in the east of Red River Fault. Based on the above discussion, it is possible that the geodynamic background of the Gejiu district changed from ~80 Ma to ~30 Ma, the former was the Late Cretaceous intraplate regional lithosphere extension in the whole western South China Block, and the latter one was influenced by the left-lateral strike-slip of Ailaoshan-Red

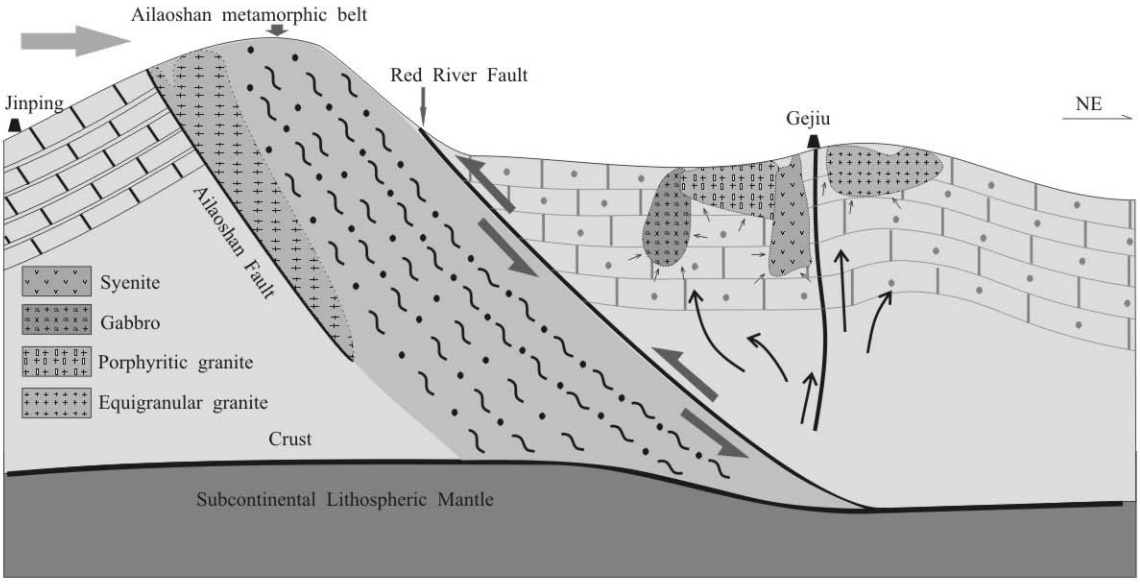

Fig. 7. Sketch map showing the geotectonic model of the Ailaoshan-Honghe and west Cathaysia area during Oligocene epoch.

River Fault, which is caused by the collision between India Plate and Euroasian continent.

6 Conclusion

Shenxianshui equigranular granite in Gejiu district, Yunnan province formed during 81±0.7 to 83±0.4 Ma, the mafic microgranular enclaves formed in 82±0.0 Ma, the enclave bearing granite formed in 81±0.5 Ma and the Jiasha gabbro formed in 80±0.2 Ma, indicating the timing of this gabbro-enclave-granite association is almost coeval in Late Cretaceous. The Late Cretaceous magmatism in western South China Block is the result of large scale lithosphere extension, and during ~30 Ma, the Gejiu district was influenced by the collision between India Plate and Euroasian continent. During ~80 Ma to ~30 Ma, the geodynamic setting of the Gejiu district experienced a great change.

Acknowledgements

We appreciate the assistance of Mr Hou Kejun with zircon U–Pb dating, Dr Zhenyu Chen with zircon CL imaging. We also want to express our thanks to Mr. Guopei Mo, Mr. Xiang Tong, Mr. Junde Wu and other local geo-workers from Yunnan Tin Group for their assistance during our field works. This study was supported by the National Science Foundation of China (40930419), Special Research Funding for the Public Benefits Sponsored by MLR (200911007–12), Research Program of Yunnan Tin Group (2010–04A), Geological Investigation Program by CGS (1212011120994), and the Fundamental Research Funds for the Central Universities (2–9–2010–21).

Manuscript received Jan. 29, 2012
accepted Mar. 29, 2012
edited by Liu Lian

References

308 Geological Party, 1984. *Geology of Gejiu tin deposits*. Beijing: Metallurgical industry publishing house, 50–90 (in Chinese).

Abdalla, J.A., Said, A.A., and Visona, D., 1996. New geochemical and petrographic data on the Gabbro-Syenite Suite between Hargeysa and Berbera-Shiikh (northern Somalia). *Journal of African Earth Sciences*, 23(3): 363–373.

Anderson, T., 2002. Correction of common lead in U-Pb analysis that do not report ^{204}Pb. *Chemical Geology*, 192: 59–79.

Barbarin, B., 1988. Field evidence for succesive mixing and mingling between the Piolard Diorite and the Saint- Julien- la-Vetre Monzogranite (Nord-Forez, Massif Central, France). *Canada Journal of Earth Science*, 25: 49–59.

Cai Minghai, He Longqing and Liu Guoqing, 2006. SHRIMP zircon U-Pb dating of the intrusive rocks in the Dachang tin - polymetallic ore district, Guangxi and their geological significance. *Geological Review*, 52, 409–414 (in Chinese with English abstract).

Castro, A., Patieo Douce, A.E., and Corretge, L.G., 1999. Origin of peraluminous granites and granodiorites, Iberian massif, Spain, an experimental test of granite petrogenesis. *Contribution to Mineralogy and Petrology*, 135: 255–276.

Cheng Yanbo, Mao Jingwen, Chen Maohong, Yang Zongxi, Feng Jiarui and Zhao Haijie, 2008b. LA-ICP-MS zircon dating of the alkaline rocks and lamprophyres in Gejiu area and its implications. *Geology of China*, 35(6): 1082–1093 (in Chinese with English abstract).

Cheng Yanbo, Mao Jingwen and Xie Guiqing, 2008a. Preliminary study of the petrogenesis of Laochang-Kafang granite in the Gejiu area, Yunnan province: Constraints from geochemistry and zircon U-Pb dating. *Acta Geologica Sinica*, 81(11): 1478–1493 (in Chinese with English abstract).

Cheng Yanbo, Mao Jingwen and Xie Guiqing, 2009. Zircon U-Pb Dating of the granites in Gejiu superginat tin polymetallic ore-field and its significance. *Mineral Deposits*, 28(3): 297–312 (in Chinese with English abstract).

Chung, S.L., Ching, H.L., Tung, Y.L., Zhang, Y.Q., Xie, Y.W., Li, X.H., Wang, K.L., and Wang, P.L., 1998. Diachronous uplift of the Tibetan plateau starting 40Myr ago. *Nature*, 394: 769–773.

Chung, S.L., 1997. Intraplate extension prior to continental extrusion along the Ailao Shan-Red River shear zone. *Geology*, 25, 311–314.

Cliff, S.J.S., 1997. The petrology of the layered gabbro intrusion, eastern gabbro, Coldwell alkaline complex, Northwestern Ontario, Canada: Evidence for multiple phases of intrusion in a ring dyke. *Lithos*, 40: 243–259.

Cong Feng, Lin Shiliang, Zou Guangfu, Xie Tao, Li Zaihui, Tang Fawei and Peng Zhimin, 2011. Geochronology and Petrogenesis for the Protolith of Biotite Plagioclase Gneiss at Lianghe, Western Yunnan. *Acta Geologica Sinca* (English edition), 85(4): 870–880.

Crofu, F., Hanchar, J.M., and Hoskin, P.W.O., 2003. Atlas of zircon textures. *Reviews in Mineralogy and Geochemistry*, 53: 469–495.

Dai Fusheng, 1996. Characteristics and evolution of rock series,lithogenesis,metallogenesis of crust-derived anatectin magma in Gejiu ore field. *Geology of Yunnan*, 15(4): 330–344 (in Chinese with English abstract).

Deng Wanming, Huang Xuan and Zhong Dalai, 1998. The relationship between alkaline porphyries and intraplate distortion in the north part of Jinshajiang belt, western Yunnan province. *Science in China* (Series D), 28(2): 111–117.

Didier, J., and Barbarin, B., 1991. *Enclaves and granite petrology*. Amsterdam: Elsevier Science, 1–88.

Gilley, L.D., Harrison, T.M., Leloup, P.H., Ryerson, F.J., Lovera, O.M., and Wang, J.H., 2003. Direct dating of left-lateral deformation along the Red River shear zone, China and Vietnam. *Journal Geophysics Research*, 108(B2): Art. No. 2127.

Grazina, S., Janina W., and Jean-Clair, D., 2003. Ferro-potassic A-type granites and related rocks in NE Poland and S Lithuania: West of the East European Craton. *Precambrian Research*, 124: 305–326.

Harrison, T.M., Leloup, P.H., Ryerson, F.J., Tapponnier, P.,

Lacassin, R., and Chen, W., 1996. Diachronous initiation of transtension along the Ailao Shan-Red River shear zone, Yunnan and Vietnam. In: Yin, A., and Harrison, T.M. (eds.), *The Tectonic Evolution of Asia*. New York: Cambridge University Press. 208–226.

Hildreth, W., 1981. Gradients in silicic magma chambers: implications for lithospheric magmatism. *Journal of Geophysical Research*, 86: 10153–10192.

Hoskin, P.O., and Ireland, T.R., 2000. Rare earth element chemistry of zircon and its use as a provenance indicator. *Geology*, 28(7): 627–630.

Jackson, S.E., Pearson, N.J., and Griffin, W.L., 2004. The application of laser ablation-inductively coupled plasma-mass spectrometer (LA-ICP-MS) to in situ U-Pb zircon geochronology. *Chemical Geology*, 211: 47–69.

Leloup, P.H., Lacassin, R., Tapponnier, R., Zhong, D., Liu, X., Zhang, L., and Ji, S., 1995. The AilaoShan-Red River shear zone (Yunnan, China), Tertiary transform boundary of Indochina. *Tectonophysics*, 251: 3–10.

Li Changnian, 2002. Review of magma mixing and mingling. *Geological Science and Technology Information*, 21(4): 49–54.

Li Jiahe, 1985. Origin and characteristics of Gejiu granites. *Yunnan Geology*, 4(4): 327–352.

Liang Huaying, Yu Hengxiang, Mo Cehui, Zhang Yuquan and Xie Yingwen, 2006. Zircon LA-ICP-MS U-Pb age, Ce^{4+}/Ce^{3+} ratios and the geochemical features of the Machangqing complex associated with copper deposit. *Chinese Journal of Geochemistry*, 25(3): 223–229.

Lin Qingcha, Xia Bin, Zhang Yuquan and Wang Yanbin, 2005. SHRIMP zircon dating on the alkaline granite in Bayi villiage, Jinping in the Ailaoshan-Jinshajiang alkaline rocks belt, Yunan province. *Geological Bulletin of China*, 24(5): 421–423.

Liu Hongying, Xia Bin and Zhang Yuquan, 2003. Study on the SHRIMP U-Pb dating on the granite porphyry in Matouwan, Yunnan province. *Acta Geoscientica Sinica* (English edition), 24(6): 552–554.

Liu Hongying, Zhang Yuquan and Xia Bin, 2004. Re-study on the Rb-Sr isotopes of the two alkaline rocks in western Yunan province. *Yunan Geology*. 23(1): 52–59.

Liu Yuping, Li Zhengxiang and Li Huiming, 2007. U-Pb geochronology of cassiterite and zircon from the Dulong Sn-Zn deposit: evidence for Cretaceous large - scale granitic magmatism and mineralization events in southeastern Yunnan province, China. *Acta Petrologica Sinica*, 23: 967–976 (in Chinese with English abstract).

Luo Junlie., 1995. The model of Sn, W, Zn, Pb, Ag deposit in southeast Yunnan Province. *Yunnan Geology*, 14(4): 319–332 (in Chinese with English abstract).

Mao Jingwen, Xie Guiqing, Guo Chunli, Yuan Shunda, Cheng Yanbo and Chen Yuchuan, 2008b. Spatial-temporal distribution of Mesozoic ore deposits in South China and their metallogenic settings. *Geological Journal of China Universities*, 14: 510–526 (in Chinese with English abstract).

Mao Jingwen, Xie Guiqing, Bierlein F. and Ye Huishou, 2008a. Tectonic implications from Re–Os dating of Mesozoic molybdenum deposits in the East Qinling–Dabie orogenic belt. *Geochimica et Cosmochimica Acta*, 72: 4607–4626.

Mao Jingwen, Xie Guiqing, Pirajno F., Ye Huishou, Wang Yanbin, Li Yongfeng, Xiang Junfeng and Zhao Haijie, 2010. Late Jurassic–Early Cretaceous granitoid magmatism in Eastern Qinling, central-eastern China: SHRIMP zircon U–Pb ages and tectonic implications. *Australian Journal of Earth Sciences*, 57: 51–78.

Mingram B., Trumbull R.B., Littman S., and Gerstenberger H., 2000. A petrogenetic study of anorogenic felsic magmatism in the Cretaceous Paresis ring complex, Namibia: Evidence for mixing of crust and mantle-derived components. *Lithos*, 54: 1–22.

Mo Xuanxue, Zhao Zhidan, Deng Jinfu, Yu Xuehui, Luo Zhaohua and Dong Guocheng, 2007. Migration of the Tibetan Cenozoic potassic volcanism and its transition to eastern basaltic province: implications for crustal and mantle flow. *Geoscience*, 21(2): 255–264.

Neves, S.P., and Vanchez, A., 1995. Successive mixing and mingling of magmas in a plutonic complex of northeast Brazil. *Lithos*, 34: 275–299.

Ratschbacher, L., Frisch, W., Chen, C., and Pan, G., 1996. Cenozoic deformation, rotation, and stress patterns in eastern Tibet and western Sichuan, China. In: Yin, A., and Harrison, T.M. (eds.), *The Tectonic Evolution of Asia*. New York: Cambridge University Press. 227–249.

Rizvanova, N.G., Lenchenkov, O.A., and Belous, A.E., 2000. Zircon reaction and stability of the U-Pb isotope system during the interaction with carbonate fluid: Experimental hydrothermal study. *Contribution to Mineralogy and Petrology*, 139: 101–134.

Song Biao, Zhang Yuhai, Wan Yusheng and Jian Ping, 2002. The SHRIMP sample manufacture, test and explaination of some phenomena for the zircon. *Geological Review*, 48(supp): 26–30 (in Chinese).

Syder, D., Carmbes, C., and Tait, S., 1997. Magma mingling in dikes and sills. *Journal of Geology*, 105: 75–86.

Tapponnier, P., Lacassin, R., Leloup, P.H., Zhong, D., Wu, H., Liu, X., Ji, S., Zhang, L.S., and Zhong, J., 1990. The Ailao Shan /Red River metamorphic belt: Tertiary left-lateral shear between Indochina and South China. *Nature*, 343: 431–437.

Tu Guangzhi, Zhang Yuquan and Zhao Zhenhua, 1984. Preliminary study on two alkaline-rich intrusion belts in South China. In: Xu Keqing and Tu Guangzhi (eds.), *Granitic geology and its relationship with mineralization*. Science and Technology Press of Jiangsu Province, 21–37 (in Chinese).

Upadhyay, D., Raith, M.M., Mezger, K., and Hammerschmidt, K., 2006. Mesoproterozoic rift-related alkaline magmatism at Elchuru, Prakasam Alkaline Province, SE India. *Lithos*, 89: 447–477.

Vavra, G., 1990. On the kinematics of zircon growth and its petrogentic significance: a cathodoluminescence study. *Contribution to Mineralogy Petrology*, 106: 90–99.

Vernon, R.H., 1983. Restite, xenoliths and microgranitoid enclaves in granites. *J. Proceed. Royal. Soc. N. S. W.,* 116: 77–103.

Wang Denghong, 2004. Dating the Dachang giant tin-polymetallic in Nandan, Guangxi. *Acta Geologica Sinica*, 78 (1): 132–138 (in Chinese with English abstract).

Wang Dezhi, Zhou Xinmin and Xu Xisheng, 1992. Origin of microgranular mafic granitic enclave. *Journal of Guilin Institute of Technology*, 12(3): 235–240.

Wang Jianghai, Yin An., Harrison M.T., Marty G., Zhang Yuquan and Xie Guanghong, 2001. A tectonic model for Cenozoic igneous activities in the eastern Indo-Asian collision

zone. *Earth and Planetary Science Letters*, 188(1–2): 123–133.

Wang Jianghai, Yin An, Harrison T.M., Grove M., Zhou Jiangyu and Xie Guanghong, 2001. Thermochronological constraints on the timing of Cenozoic high-potassic magmatism in eastern Tibet. *Bulletin of Mineralogy, Petrology and Geochemistry*, 20(4): 231–233.

Wang Xinguang, Zhu Jinchu and Shen Weizhou, 1990. Contrast study on two main ore-forming granites in Gejiu tin deposit and their geological and prospecting significance. *Journal of Nanjing University* (Earth Science Edition), 4: 66–75.

Wang Xingzhen, 2006. *Origin and geochemistry of the Gejiu complex*. Master thesis of Institute of Geochemistry, Chinese Academy of Sciences, 1–76 (in Chinese with English abstract).

Wilcox, R.E., 1999. The idea of magma mixing: history of a struggle for acceptance. *The Journal of Geology*, 107: 421–432.

Williams, I.S., 1992. Some observations on the use of zircon U-Pb geochronology on the study of granitic rocks. *Trans. Royal Soc. Edinburgh: Earth Sci.*, 83: 447–458.

Wu Qingsheng, Xu Junzhen and Yang Zhi, 1984. Study on Sr isotope character and prospecting criteria of tin-bearing granite of Gejiu area. *Geochemica*, 4: 293–302.

Wu Yuanbao and Zheng Yongfei, 2004. Genetic mineralogy of zircon and contraints on the explaination of U-Pb ages. *Chinese Scinence Bulletin*, 49(16): 1589–1604 (in Chinese).

Xia Bin, Lin Qingcha and Zhang Yuquan, 2005. SHRIMP zircon U-Pb dating of granite in Ailaoshan-Jinshajiang belt and significance: a case study of Yuzhaokuai, Matouwan and Shilicun stocks. *Geotectonica et Metallogenia*, 29(1): 35–43.

Xia Bin, Li Jianfeng, Xu Lifeng, Wang Ran and Yang Zhiqing, 2011. Sensitive High Resolution Ion Micro-Probe U-Pb Zircon Geochronology and Geochemistry of Mafic Rocks from the Pulan-Xiangquanhe Ophiolite, Tibet: Constraints on the Evolution of the Neo-tethys. *Acta Geologica Sinca* (English edition), 85(4): 840-854.

Xie Yingwen and Zhang Yuquan, 1984. A preliminary study on geochemical characteristics and mineralization specificity of alkali-rich intrusive belt in Ailaoshan-Jinshajiang. *Journal of Kunming College of technology*, 85(4): 1–17.

Yang Zongxi, Mao Jingwen and Chen Maohong, 2009. ^{40}Ar-^{39}Ar dating of muscovite from Laochang veinlet like Sn deposit in Gejiu tin polymetallic ore district and its geological significance. *Mineral deposits*, 28(3): 336–344.

Yang Zongxi, Mao Jingwen and Chen Maohong, 2008. Re-Os dating of molybdenite from the Kafang skarn copper (tin) deposit in the Gejiu tin polymetallic ore district and its geological significance. *Acta Petrologica Sinica*, 24(8): 1937–1944.

Yu Chongwen, Tang Yuanjun and Shi Pingfang, 1988. *The denamic system of endogenic ore formation in Gejiu tin-polymetallic ore region, Yunnan province*. Wuhan: China University of Geosciences Press, 42–251 (in Chinese).

Zhang Hongpei, Liu Jishun, Li Xiaobo and Zhang Xialin, 2006. The relationship between the granites and Sn, Ag, Cu, Pb, Zn polymetallic deposits in southeast Yunnan province. *Contributions to Geology and Mineral Resources Research*, 21(2): 87–90 (in Chinese with English abstract).

Zhang Yuquan and Xie Yingwen, 1997. Geochronology of Ailaoshan-Jinshajing alkali-rich intrusive rocks and their Sr and Nd isotopic characteristics. *Science in China* (Series D), 26(4): 289–293.

Zhuang Yongqiu, Wang Renzhong and Yang Shupei, 1996. *Tin-copper polymetallic deposit*. Beijing: Earthquake publishing house, 38–101 (in Chinese).